A WRINKLED MOON T. J. Thompson[1], M. S. Robinson[1], T. R. Watters[2] [1]Lunar Reconnaissance Orbiter Camera, School of Earth and Space Exploration, Arizona State University, Tempe, AZ, USA; [2]Center for Earth and Planetary Studies, National Air and Space Museum, Smithsonian Institution, Washington, DC 20560, USA. (tthompson@ser.asu.edu);

Introduction: Wrinkle ridges are tectonic landforms characterized by linear topographic highs with complicated surface expressions involving a broad arch and a sharp ridge interpreted as the result of thrust faulting from comparison with earth analogs [1, 2]. These features were discovered through telescopic observations of the Moon [3], and were later found on several terrestrial bodies by observing spacecraft [2, 4]. Lunar wrinkle ridges are concentrated in the mare basalts of the Moon's nearside (Figure 1). The question of why wrinkle ridges are confined to mare basalts is partially addressed in the mascon tectonic model in which impact basins are filled with approximately 4 kilometers of basalt denser than the average lunar crust, causing an adjustment in the crust to accommodate the added mass, where this accommodation generates the compressional stress necessary to form wrinkle ridges [5, 6, 7, 8, 9].

In previous work, the lunar wrinkle ridges were digitized using wide angle camera (WAC) products [10] from the Lunar Reconnaissance Orbiter Camera (LROC) team [11]. This wrinkle ridges shapefile dataset, the lunar mare shapefile [12], and Gravity Recovery and Interior Laboratory (GRAIL) Bouguer gravity anomaly data derived from the GRGM900C [13] are explored in this study comparing wrinkle ridge orientations across the lunar maria. We compare these areas in terms of the the orientations of wrinkle ridges, gravity features, and mare boundaries.

Methods: For comparative orientation of lines within a bounding shape, a Python script was written to split polylines into individual two-node segments and compare the orientation of those segments to the nearest segment on the bounding polygon. The reported angle is the difference in degrees, with a range of 0 to 90, between the ridge segment and the closest segment on the bounding polygon.

Orientations: Splitting the wrinkle ridges into their individual ridge segments (two-node pairs) results in over 42,000 segments for orientation calculations. Comparison to the polygons bounding the wrinkle ridges shows that a greater number of segments are $<= 45°$ from the near edge of the polygon compared to $> 45°$. Also evident, there is abundant randomness in the dataset, some of which may result from the irregular nature of the bounding polygon. However, looking at the map locations (Figure 1) of the [0 to 10] and [80 to 90] angular difference bins shows these features show some degree of organization. For instance, features in the [0 to 10] bin tend to be located near other features in that bin, and likewise for [80 to 90].

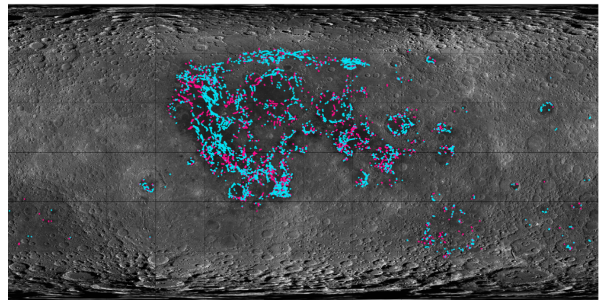

Figure 1: Global map of orientations of wrinkle ridges compared to nearest spot on the bounding mare boundary. Light blue features are selected as being 10 degrees or less different than the near segment on the boundary. Pink features are selected as being 80 or more degrees different than the near segment on the boundary.

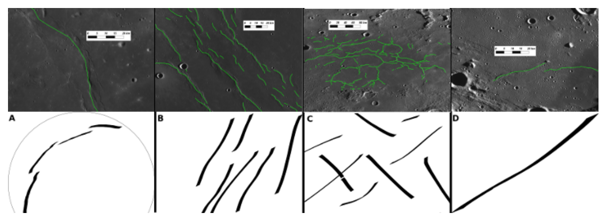

Figure 2: Specific lunar examples (top row) and diagram of several types of wrinkle ridge patterns. A) Arcuate coherent, collection of lines tightly follow a curve. B) Linear coherent, a grouping of lines share a similar strike. C) Linear noncoherent, the grouping of lines do not follow a similar strike, often 2 directions. D) Linear isolated, individual lines with few neighbors, such as occurs with ridges in very small mare patches.

Visual Inspection: Wrinkle ridges were classified based on the orientation of features around them (Figure 2). The features described as concentric in the basins of Crisium, Nectaris, Serenitatis, Imbrium, Humorum, and Orientale appear to occur in sets building a curve when taken in aggregate. Each segment is likely straight, but a slight angle between successive features contributes to the broad appearance of a curve. These features appear near the boundary of positive Bouguer gravity anomalies, and also associated mare depth gradient according to thickness maps generated from partially filled mare craters [14, 15].

In many cases wrinkle ridges are located nearby and sometimes of similar shape to positive GRAIL Bouguer gravity anomalies. This case is particularly evident in

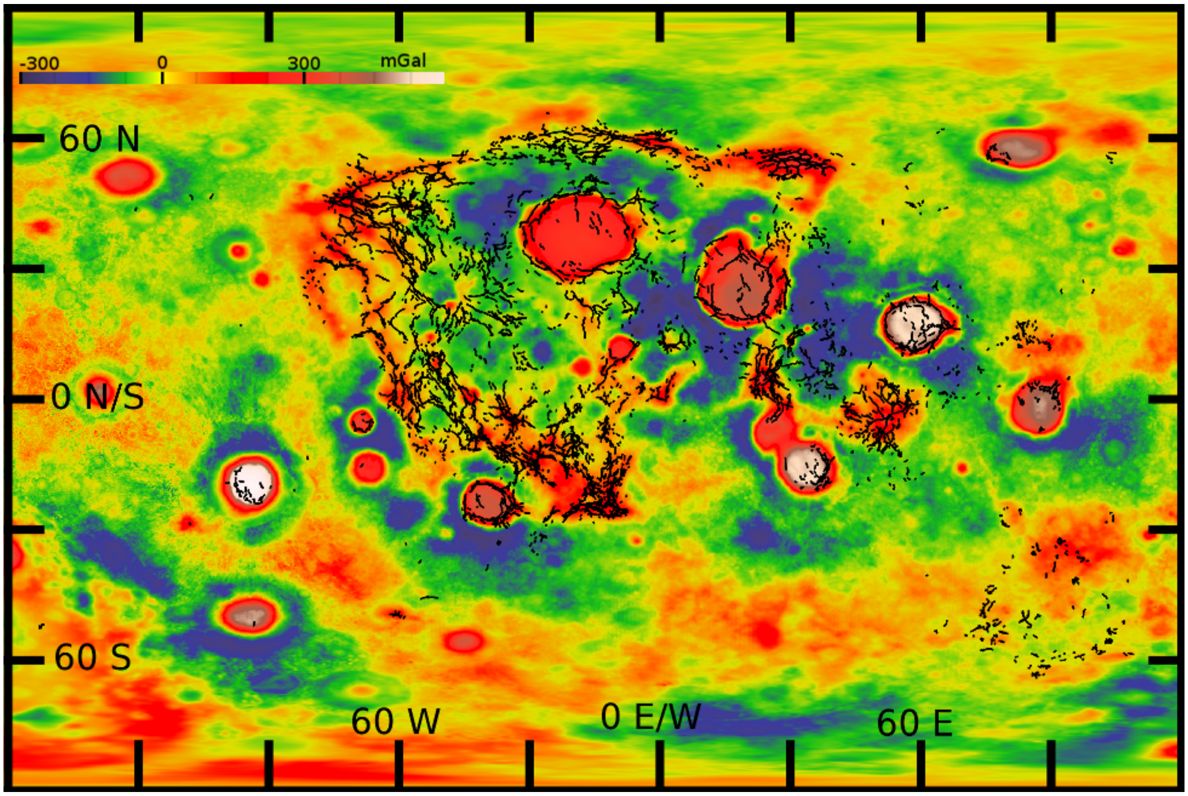

Figure 3: Lunar wrinkle ridges (fine black lines) atop degree 6-660 filtered Bouguer gravity anomalies derived from GRAIL data

the circular basins of Crisium, Nectaris, Serenitatis, Imbrium, Humorum, and Orientale (Figure 3). The concentric wrinkle ridges appear positioned near the gravity gradient. Just a few radial features cut through the bulk of the positive anomaly itself in the center of the basin.

The other set of ridges showing organization are sets of parallel lines occurring in groups, called "linear coherent"(Figure 2B). These features can be found in northwest Oceanus Procellarum. In this region the mare is shallow [15] and the positive anomalies are similarly oriented [16]. Areas of Mare Frigoris also exhibit this alignment between positive Bouguer anomaly and ridge strike.

Isolated ridges have no nearby features and thus fall into their own linear isolated classification (Figure 2D). Groupings of ridges which show at least two evident strike directions (Figure 2C) also exist. These features may be found in far-north Procellarum near Frigoris, where there appears to be a change in trend. In far-east Frigoris, the two different strikes produce a polygonal appearance. These "incoherent linear" groupings are distributed throughout the positive gravity anomaly, while the "arcuate coherent" were distributed near the edge of the anomalies. In the case of Nubium and Cognitum, the mare is thinner according to the mare thickness isopach maps by De Hon [15], and there are nearby exposures of non-mare material indicating the presence of perhaps complicated sub-mare topography.

Discussion: Groupings of wrinkle ridges within the mare show strong correlation with the orientation of the mare boundaries, particularly in the non-mascon mare of Procellarum and Frigoris. In the roughly circular mare, the wrinkle ridges are consistent with fault trajectories predicted in the mascon tectonic model. Orientation agreement between the ridges and mare in the non-mascon could relate to the shape and geometry of regional-scale lowlands the mare basalts occupy [17].

References: [1] J. B. Plescia, et al. (1986) *GSA Bulletin* 97(11):1289. [2] T. R. Watters (1988) *JGR* 93(B9):10236. [3] G. Gilbert (1893) *Washington Bull* 12:241. [4] T. R. Watters (1992) *Geology* 20(7):609. [5] R. J. Phillips, et al. (1972) *JGR* 77(35):7106. [6] W. B. Bryan (1973) in *4th LPSC*. [7] S. C. Solomon, et al. (1979) *JGR*. [8] S. C. Solomon, et al. (1980) *Reviews of Geophysics* 18(1):107. [9] A. M. Freed, et al. (2001) *JGR*. [10] R. V. Wagner, et al. (2015) in *46th LPSC*. [11] T. J. Thompson, et al. (2017) in *48th LPSC*. [12] D. Nelson, et al. (2014) in *45th LPSC*. [13] F. G. Lemoine, et al. (2014) *Geophysical Research Letters* 41(10):3382. [14] R. A. Dehon, et al. (1976) in *7th LPSC*. [15] *NASA Technical Report NASA-CR-158784*. [16] D. H. Scott (1974) in *5th LPSC* 3025–3036. [17] T. R. Watters, et al. (2010) *Planetary Tectonics* Cambridge University Press.